2010 MRS FALL MEETING

Facile Synthesis of Polypyrrole/Graphene Nanosheet-based Nanocomposites as Catalyst Support for Fuel Cells.

Journal:	*2010 MRS Fall Meeting*
Manuscript ID:	MRSF10-1312-II12-08.R1
Manuscript Type:	Symposium II
Date Submitted by the Author:	n/a
Complete List of Authors:	Saner, Burcu; Sabanci University, Materials Science and Engineering Alkan Gürsel, Selmiye; Sabanci University, Materials Science and Engineering Yürüm, Yuda; Sabanci University, Materials Science and Engineering
Keywords:	chemical reaction, polymerization, surface chemistry

Facile synthesis of polypyrrole/graphene nanosheet-based nanocomposites as catalyst support for fuel cells

Burcu Saner, Selmiye Alkan Gürsel and Yuda Yürüm
Faculty of Engineering and Natural Sciences, Sabanci University Orhanli, Tuzla, Istanbul 34956, Turkey

ABSTRACT

The integration of catalyst metals into the graphene-based composites can be a new way to ensure thermal and electronic conductivities of the catalyst support materials in polymer electrolyte membrane fuel cells. In this work, graphene nanosheets were synthesized via a mild and safer chemical route including three major steps: graphite oxidation, ultrasonic treatment and chemical reduction. Then, polypyrrole was coated on graphene nanosheets by *in-situ* polymerization to fabricate polypyrrole/graphene nanosheet-based nanocomposites as the catalyst supports. Pt nanoparticles were uniformly dispersed on the surface of nanocomposites by sonication technique.

INTRODUCTION

Polymer nanocomposites incorporating carbon black, carbon nanotubes, and carbon nanofibers have been utilized for improved mechanical, thermal, electrical and gas barrier properties of polymers especially in the field of energy storage and electronics [1]. Recently, graphene sheets are promising materials to be used as nanofillers in the polymer matrices due to their high electrical conductivity, excellent mechanical strength, high surface area and high chemical stability [2]. Graphene is a single flat monolayer of sp^2-carbon atoms in 2D crystal structure. With the proper surface modifications, single graphene sheets can be separated from the graphite material and the layer-to-layer distance can be extended [3]. Chemical exfoliation is one of the extensively used methods to break van der Waals forces between graphene sheets in graphite and to receive monolayer graphene sheet.

In fuel cells, the catalyst layer must be very effective at breaking molecules into protons and electrons have high surface area, adequate porosity, high electronic conductivity, and it should be chemically and mechanically stable [4]. Catalyst has a great effect on both the cost and durability of polymer electrolyte membrane fuel cells (PEMFCs). In PEMFCs, platinum (Pt) can be considered as the best electrocatalyst in acidic media since it serves the lowest overpotentials and the highest activity [5]. Conducting polymers, especially polypyrrole (PPy), are widely preferred for fuel cell operations because of good electronic and proton conductivity, and dispensability [6]. PPy-modification can increase the electrochemical surface area and enhance the electrocatalysis ability of Pt/carbon catalyst [7].

In present work, graphene nanosheets as nanofillers were reinforced in polypyrrole by *in situ* polymerization to be used as the catalyst support material. In these nanocomposites, graphene sheets act as electron acceptors while PPy serves as an electron donor. Graphene nanosheets were exfoliated from graphite flakes in large amounts by applying a mild and safer method. The distribution and the size of Pt nanoparticles on the surface of composites were investigated to understand the importance of deposition technique.

EXPERIMENT

Chemical exfoliation of graphene nanosheets

Graphene nanosheets were produced by a safer and mild chemical route consists of oxidation, ultrasonic treatment and chemical reduction in large quantities [8]. Potassium permanganate ($KMnO_4$) is mostly used as an oxidizing agent in oxidation process but this chemical is very severe and leads to explosions when it is used together with H_2SO_4. Hence, potassium dichromate ($K_2Cr_2O_7$) was used as a milder oxidant in order to reduce the risks. In graphite oxidation, graphite flakes (1 g) was added into chromic acid prepared by using potassium dichromate, sulfuric acid and distilled water and then acetic anhydride (1 g) was poured dropwise into the mixture and the mixture was stirred at 45 ^oC for 10 days. The amounts of $K_2Cr_2O_7$ and H_2SO_4 were adjusted in the weight ratio 2.1:55. Filtration and neutralization of samples were conducted by using 0.1 M NaOH and distilled water until washings were neutralized. After oxidation process, ultrasonic treatment was performed for the homogenous dispersion of graphite oxide (GO) sheets. At last, sonicated GO sheets were chemically reduced through refluxing with hydroquinone in water to produce graphene nanosheets.

Synthesis of PPy/graphene nanosheet-based nanocomposites

PPy was coated on graphene nanosheets by *in situ* polymerization of pyrrole (Py) using $FeCl_3$ as the oxidant in the mixture of H_2O and ethanol in 1:1 (v/v) at room temperature for 24 hr [9]. The Fe^{3+}/Py molar ratio was approximately 2.4 [10]. The precipitated sample was filtered and rinsed several times by ethanol and distilled water to remove excess Py, catalyst and side products. The black powder was dried overnight in a vacuum oven at $60^{\circ}C$. The feeding mass ratio of Py and graphene nanosheets was adjusted as 1:1.

Pt nanoparticle deposition on nanocomposites

Pt deposition on the surface of composites was conducted by applying sonication technique. At first, graphene nanosheets were exposed to ultrasonic vibration for the homogeneous dispersion of sheets, and 8 % H_2PtCl_6 solution was added into mixture, and then 1 M $NaBH_4$ as a reducing agent was poured into mixture, respectively. The deposition time was adjusted to 2 hr.

All samples were characterized by Scanning Electron Microscopy (SEM), X-Ray Diffraction (XRD), Thermal Gravimetric Analyzer (TGA), Atomic Force Microscope (AFM), Raman spectroscopy and surface area analyzer. The electrical conductivities of pellet electrodes were measured by a conventional four-probe method at room temperature.

DISCUSSION

Graphene nanosheets

Pristine graphite contained smooth and sharp layers as shown in Figure 1 a. The oxidation process led to the formation of expanded and ripple structure as shown in Figure 1 b. During the oxidation, acetic anhydride diffused into layers and layers started to extend.

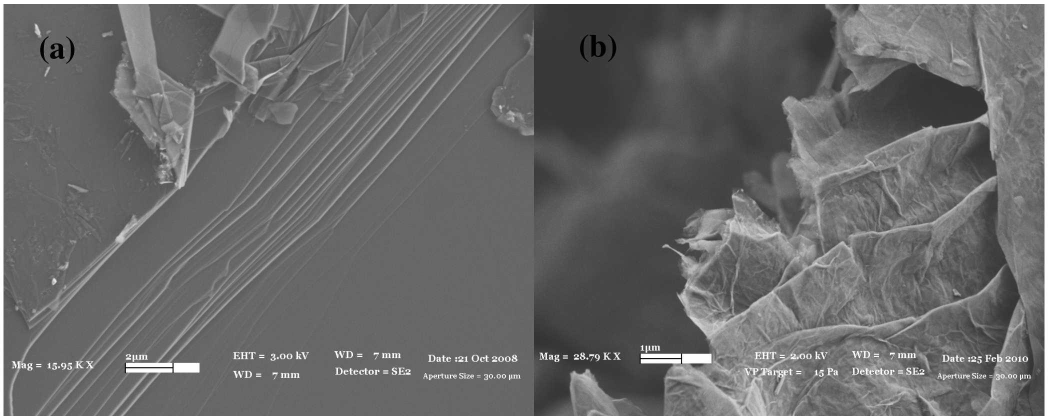

Figure 1. SEM images of **(a)** graphite flakes and **(b)** partially oxidized GO sheets

The XRD pattern of pristine graphite had a very sharp and high intense 002 peak but the intensity of this peak decreased comparably due to the destruction of structure (Figure 2 a and 2 b). Furthermore, the change of crystal structure can be estimated by using XRD data by applying Debye Scherrer equations [11]:

$$L_a = 0.89\lambda / \beta_{002} \cos\theta_{002} \quad (1)$$

$$n = L_a / d_{002} \quad (2)$$

(**L_a** **:** stacking height, **β** **:** full width half maxima (FWHM), **n:** average number of graphene layers, **d_{002}** **:** interlayer spacing). Average number of graphene layers for pristine graphite and GO sheets were estimated as 86 and 21, respectively. This also revealed how oxidation process destruct the graphitic structure.

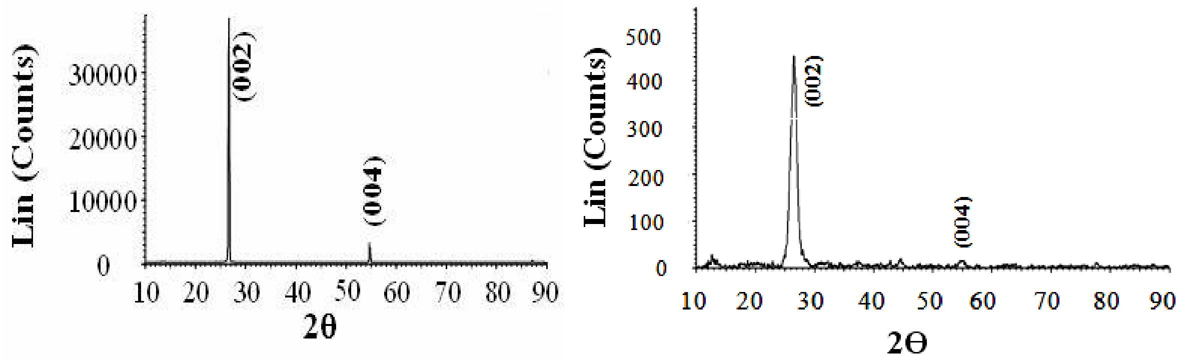

Figure 2. XRD patterns of **(a)** pristine graphite and **(b)** partially oxidized GO sheets

After ultrasonic treatment of GO sheets, samples were reduced by using hydroquinone in order to receive graphene nanosheets, Figure 2. There are several attempts in literature to separate graphene nanosheets from graphite. Herein, there are two distinct differences which are a milder oxidant and a simplified and cost effective procedure. Graphene nanosheets can be produced in large quantities to be used as the nanofillers in polymer composites.

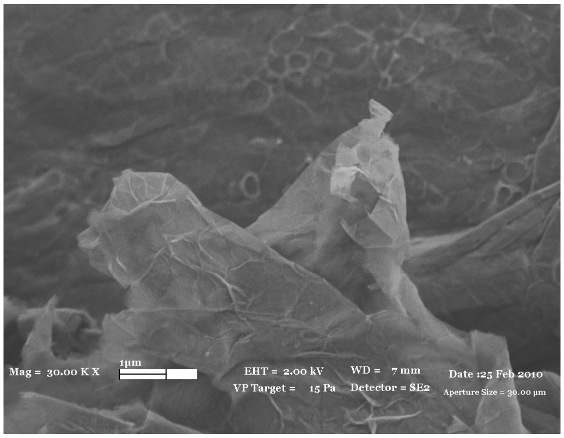

Figure 2. SEM image of graphene nanosheets after chemical reduction

PPy/Graphene nanosheet-based nanocomposites

Py as a monomer diffused into graphene nanosheets during *in situ* polymerization and polymerized on the surface of graphene nanosheets layer by layer. Figure 3 depicted the successful layer by layer coating and sphere-like morphology of PPy particles. In this composite, graphene sheets act as electron acceptors while PPy serves as an electron donor.

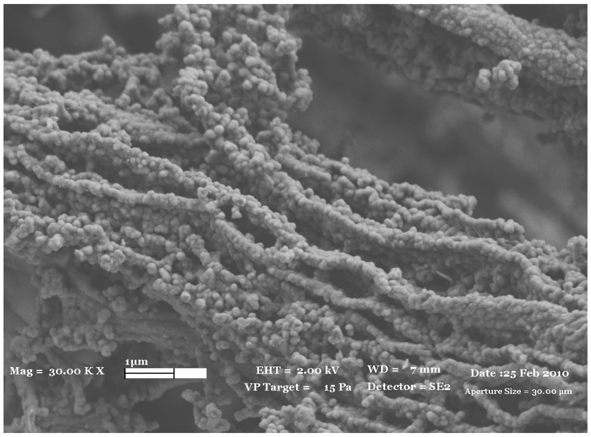

Figure 3. SEM image of PPy/graphene nanosheet-based nanocomposite

Raman spectroscopy is an efficient technique to estimate the layer numbers and observe the change of crystal structure. All measurements were conducted using a 514 nm argon ion laser. There are three distinct peaks in Raman spectrum of graphene nanosheets which are the D band around 1364 cm^{-1}, the G band around 1582 cm^{-1} and the 2D band around 2709 cm^{-1}, Figure 4. G band intensity is directly proportional to crystallite size, La [12]. After coating PPy on the surface of graphene nanosheets, G band was broadened and its intensity was increased. This showed that crystallite size of structure was increased due to coating.

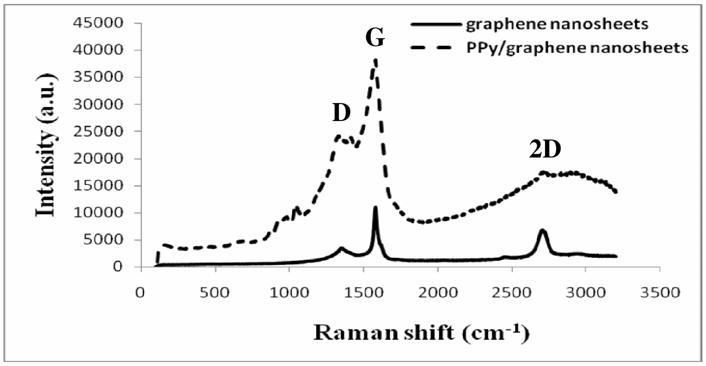

Figure 4. Raman spectra of graphene nanosheets and PPy/graphene nanosheets

The electrical conductivity of samples in the pellet form was measured by a conventional four-probe method. Conductivity of pristine PPy was relatively poor because of weak compactness and weak orientation of PPy particles [13] but conductivity was enhanced by using graphene sheets as filler in polymer matrix (Table I).

Table I. Electrical conductivities of PPy, graphene nanosheets and PPy/graphene nanosheet composites

Electrodes	Conductivity (S/cm)
Pristine PPy	0.00076
Graphene nanosheets	1.5
PPy/graphene nanosheet composites	0.13

High surface area has a significant influence on the dispersion and distribution of catalytic metals on catalyst supports. Nitrogen adsorption isotherms exhibited that BET surface area of reduced GO sheets was 507 m^2/g and after coating BET surface area decreased down to 290 m^2/g.

Pt/PPy/Graphene nanosheet composites

The particle size of Pt might be correlated with the degree oxidation of graphite which means that the efficient deposition of Pt nanoparticles is due to the strong interaction between the metal salt precursor and the functional group of GO sheets [14]. Herein, functionalized graphene nanosheets after 10 days of oxidation acting as the metal-anchoring sites provide metal nuclei formation and electrocatalysts deposition. During Pt deposition on graphene nanosheets, some Pt particles were aggregrated and some of them were dispersed uniformly on the surface. Figure 5 a exhibited that Pt particles were aggregated during deposition of Pt on the surface of graphene nanosheets. However, uniform dispersion of Pt particles was observed when graphene sheets were coated by PPy, Figure 5 b. This indicated a strong interaction between support and catalyst particles. Size distribution of Pt particles on the surface of the nanocomposites changed from 20 nm to 30 nm. Furthermore, sonication process provided the best exfoliation and dispersion of both Pt nanoparticles and graphene nanosheets.

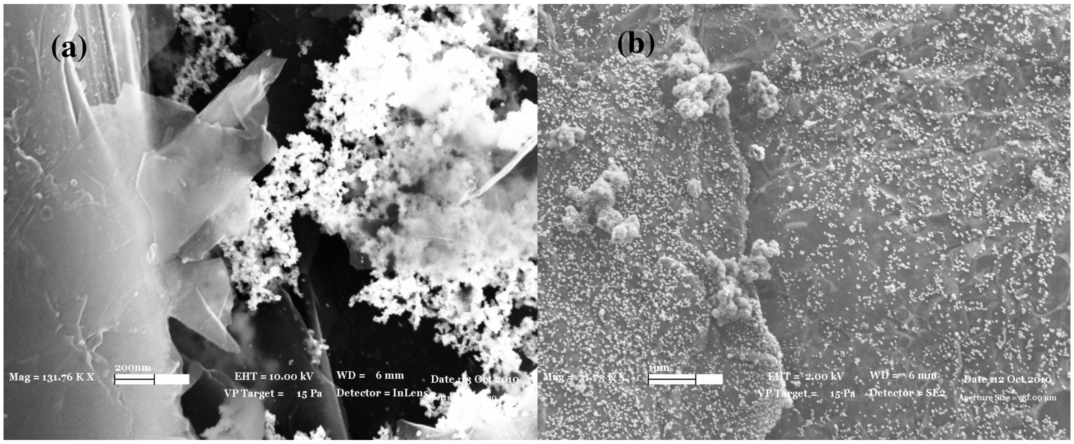

Figure 5. SEM images of **(a)** Pt/graphene nanosheets via inlens detector and **(b)** Pt/PPy/graphene nanosheets via secondary electron detector

CONCLUSIONS

Graphene nanosheets were exfoliated from graphite by applying a mild and cost effective chemical route including oxidation, sonication and reduction. Graphene nanosheets based nanocomposites were prepared by a layer-by-layer PPy coating by *in situ* polymerization of Py monomer. The incorporation of graphene sheets in polymer matrix provided uniform dispersion of Pt nanoparticles on the surface with the help of sonication process. The support material has great importance to achieve high catalytic activity of fuel cell catalyst by lowering the catalyst deposition. Therefore, PPy/Graphene nanosheet-based nanocomposites having enhanced thermal stability, and electrical conductivity, and high surface can be a good alternative to carbon black and utilized as a catalyst support for Pt in PEMFCs.

REFERENCES

1. H. Kim, A. A. Abdala, and C. W. Macosko, *Macromolecules* **43**, 6515–6530 (2010).
2. S. Stankovich, D. A. Dikin, G. H. B. Dommett, et al., *Nature* **442**, 282-286 (2006).
3. M. J. McAllister, et al., *Chem. Mater.* **19**, 4396 (2007).
4. S.Natarajan and J.Hamelin, *Journal of The Electrochemical Society* **156**, B210-B215 (2009).
5. H. A. Gasteiger, S. S. Kocha, B. Sompalli, F. T. Wagner, *Appl. Catal. B.* **56**, 9 (2005).
6. R. Dersch, M. Steinhart, U. Boudriot, A. Greiner, J.H.Wendorff, *Polym. Adv. Technol.***16**, 276 (2005).
7. H. Zhao, L. Li, J. Yang, Y. Zhang, *Journal of Power Sources* **184**, 375 (2008).
8. B. Saner, F. Okyay, Y. Yürüm, *Fuel* **89**, 1903–1910 (2010).
9. T. V. Vernitskaya, O. N. Efimov, *Russian Chemical Reviews* **66**, 443-457 (1997).
10. S. P. Armes, *Synth. Met.* **20**, 365-371 (1987).
11. B. Sakintuna, S. Cetinkaya, Y. Yürüm, *Energy Fuels* **18**, 883–888 (2004).
12. K. Sato, R. Saito, et al., *Chemical Physics Letters* **427**, 117–121 (2006).
13. N. G. Sahoo, Y. C. Jung, H. H. So, J. W. Cho, *Synth. Met.* **157**, 374-379 (2007).
14. N. Rajalakshmi, H. Ryu, M. M. Shaijumon, S. Ramaprabhu, *J. Power Sources* **140**, 250–257 (2005).